

# IMPACT OF ELECTRON BEAM HEATING ON INSERTION DEVICES AT DIAMOND LIGHT SOURCE

E. C. M. Rial and Z. Patel, Diamond Light Source, Didcot, UK

## Abstract

Electron beam heating is a widely observed phenomenon at synchrotron facilities around the world, and has a large impact particularly on cryogenic insertion devices, but also on room temperature devices. This paper seeks to outline electron beam heating measurements taken at Diamond Light Source (DLS) and produces an empirical heat load relationship that matches the form of heating through the anomalous skin effect, although gives an order of magnitude higher than that predicted by theory. Resistive wall heating should vary inversely with the gap of installed cryogenic and permanent magnet insertion devices. This is also examined in this paper and the results presented.

## INTRODUCTION

We have previously reported on the electron beam heating effects on our two Superconducting Wigglers (SCWs) and our Cryogenic Permanent Magnet Undulator (CPMU) [1, 2]. In recent years we have also witnessed large temperature rises in some of our standard in-vacuum systems.

We now have over six years operational experience with our installed CPMU and SCWs, and with it a wealth of additional data with which to analyse the relationship of heat load on cryogenic devices with varying beam conditions. The relationship between the heat load on the wigglers and the electron beam has been determined to strongly correlate with bunch length; a finding supported by modifying the electron bunch length through RF Voltage, bunch charge, and the field of other installed insertion devices [2].

## ASSESSMENT OF THE SUPERCONDUCTING WIGGLERS

At the last update of the DLS Wigglers in 2011 [2], modifications had been made to the cryostats by the Budker Institute of Nuclear Physics (BINP) to improve their efficiency. This led to the elimination of liquid helium boil-off, previously a total of 4 litres/hour. Although the elimination of liquid helium boil-off was a great success, the resulting sub-atmospheric pressure of the liquid helium baths caused several problems due to the ingress of water and nitrogen ice. The cryostats were not as leak tight as they needed to be. The response to this was to implement a control system to energise the installed magnet heater to boil just enough of the helium bath to maintain an internal absolute pressure of 1040 mbar.

### Measuring Heat Load

Measuring the heat load within the superconducting wigglers is straightforward. The temperature at each stage of the coldheads is known and can be converted to power extraction

through manufacturers heat maps, e.g. [3]. In addition, any helium lost is measured with a flow meter and the amount of power required to produce that flow can be calculated. Finally the amount of power put in to the wiggler to maintain the internal pressure at 1040 mbar is monitored. Taking the general environmental heat load as a constant allows the amount of power deposited into the cryostat by the electron beam to be deduced:  $P_{\text{beam heating}} = P_{\text{coldheads}} + P_{\text{He flow}} - P_{\text{mag. heater}} - P_{\text{env. heat}}$ . Plotting  $P_{\text{beam heating}}$  against something as crude as beam current is not informative, as the headline figure of stored current in a storage ring hides significant detail about the structure of the beam. The average current,  $I_{\text{av}}$ , is not a continuous stream of electrons but rather a series of electron bunches of charge  $Q_b$ :  $I_{\text{av}} = f_{\text{rev}} \sum_b Q_b$ , where  $f_{\text{rev}}$  is the revolution frequency of the storage ring (533.8 kHz for the DLS Storage ring). If each bunch has a Gaussian shape then the frequency spectrum  $\tilde{\lambda}(\omega)$  is given by:

$$\tilde{\lambda}(\omega) = \frac{1}{c} \exp\left(\frac{-\omega^2 \sigma_b^2}{2c^2}\right) \quad (1)$$

where  $c$  is the speed of light,  $\sigma_b$  is the bunch length, and  $\omega$  is the angular frequency of an applied alternating magnetic field, from the assumption that the frequencies arising from the Fourier transform of the bunch shape are transmitted along the vessel as alternating currents.

### The Normal and Anomalous Skin Effects and Resistive Wall Heating

The result by Piwinski [4] shows that the image current in a cylinder of radius,  $r$ , is equivalent to the image current in a pair of infinite parallel plates separated by  $2r$ . When the mean free path of the conduction electrons,  $l$ , is shorter than the skin depth,  $\delta$ , the conductor is modelled using the normal skin effect (NSE). Where  $l$  is longer than  $\delta$ , the conductor is modelled using the anomalous skin effect (ASE) [5, 6]. The power,  $P$ , per unit length,  $L$ , due to resistive wall heating from a current of  $n$  bunches in a cylindrical vessel of radius  $r$  is:

$$\frac{P}{L} = \frac{n f_{\text{rev}} Q_b^2 c^2}{2\pi^2 r} \int_0^{\text{inf}} \tilde{\lambda}^2(\omega) R_s(\omega) d\omega \quad (2)$$

where the surface resistivity,  $R_s$ , is:

$$R_s(\omega) = \begin{cases} R_S^N(\omega), & l < \delta \\ R_S^A(\omega), & l > \delta \end{cases} \quad (3)$$

Using the Gamma function identity this can be expanded to:

$$\frac{P^N}{L} = \frac{n f_{\text{rev}} Q_b^2}{2\pi^2 r} \sqrt{\frac{\mu_0 \rho}{2}} \frac{1}{2} \left(\frac{c}{\sigma_b}\right)^{\frac{3}{2}} \Gamma\left(\frac{3}{4}\right) \quad (4)$$

in the NSE regime and:

$$\begin{aligned} \frac{P^A}{L} = & \frac{n f_{\text{rev}} Q_b^2}{2\pi^2 r} \left(\frac{\sqrt{3}}{16\pi} \rho l \mu_0^2\right)^{\frac{1}{3}} \left[\frac{1}{2} \left(\frac{c}{\sigma_b}\right)^{\frac{5}{3}} \Gamma\left(\frac{5}{6}\right) \right. \\ & \left. + 1.157 \left(\frac{3}{4} \frac{\mu_0 l^2}{\rho}\right)^{-\frac{69}{250}} \left(\frac{c}{\sigma_b}\right)^{\frac{1043}{750}} \Gamma\left(\frac{1043}{1500}\right) \right] \quad (5) \end{aligned}$$

in the ASE regime, where  $\mu_0$  is the permeability of free space,  $\rho$  is the resistivity of the conductor, and  $\Gamma$  is the Gamma function. Each of the skin effect regimes (NSE and ASE) is described by a slightly different inverse relationship with bunch length, summarised in Table 1.

Table 1: Relationship Between Beam Heating and Bunch Length for Different Skin Effects

Skin Effect Regime	Relation with bunch length, $\sigma_b$
NSE	$\sigma_b^{-\frac{3}{2}}$
ASE	$\sigma_b^{-\frac{1}{3}} + 2.43\sigma_b^{-1.39}$

By finding the inverse power of the bunch length relationship that best fits the data, it should in principle be possible to deduce which skin effect regime is in place.

It has been established that mean ring current is not a suitable parameter against which to assess beam heating. Instead, the sum of the squares of the bunch charges (SOCS) is more appropriate: the  $nQ_b^2$  term in Eq. (4) and Eq. (5). If the ID beam foils are approximated as infinite sheets, the heat load should vary with SOCS, electron bunch length, and ID gap, according to the power relationships.

### Electron Beam Parameters

A more appropriate parameter to assess beam heating is SOCS modified by an inverse power of bunch length  $\sigma_b$  according to the relationships in Table 1. Bunch length is not an archived parameter, however, measurements have been taken of the relationship of bunch length with bunch charge, and to confirm the relationship between bunch length and RF cavity voltages ( $\Delta V_{RF}$ ) [7]. Insertion devices also have an impact on the bunch length. The SCWs are the two IDs that most significantly impact the bunch length [8]. Multiplying these terms together allows an estimation of bunch length according to:

$$\begin{aligned} \bar{\sigma}_b(\Delta V_{RF}, \bar{Q}_b, B_W) &= \sigma_{b0} f_1(\Delta V_{RF}) f_2(\bar{Q}_b) f_3(B_W) \\ &= \sigma_{b0} \frac{1 + 0.53 \bar{Q}_b}{\sqrt{1 + \frac{\Delta V_{RF} [MV]}{2.5 MV}}} \sqrt{\frac{1 + \frac{4}{3\pi} \frac{\rho^3}{2\pi\rho} \sum \frac{L_W}{W} \rho_W^3}{1 + \frac{1}{2} \frac{\rho^2}{2\pi\rho} \sum \frac{L_W}{W} \rho_W^2}} \quad (6) \end{aligned}$$

where  $B_W$  is the wiggler fields,  $\sigma_{b0}$  is the natural bunch length (3.18 mm),  $\rho_{BM}$  and  $\rho_W$  are the bending radii of the storage ring bending magnets and the SCWs respectively, and  $L_W$  is the magnetic length of the wigglers.

### Results from the I12 and I15 Wigglers

NSE and the ASE models have been applied to the I12 and I15 wiggler data. There is a strong correlation between the heat load and SOCS that is further improved when including the ASE bunch length relationship as shown in Fig. 1. It is clear that beam heating has a dependence on SOCS and bunch length, however, it is not clear from the bunch length if the NSE or ASE model is more appropriate. Despite the resistive wall heating effect the data shows, the measured heat load is significantly above the theoretical prediction, as shown in Table 2.

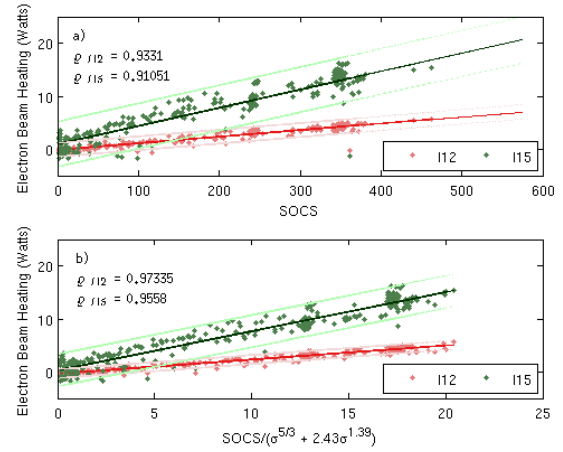


Figure 1: Heat load vs. (a) SOCS and (b) modified SOCS to include the ASE bunch length relation for the I12 and I15 wigglers. The correlation coefficients improve when the bunch length relationship is included.

## ASSESSMENT OF THE CPMU

The measurement of the heat deposited in the CPMU is a more direct affair. Due to the nature of the NdFeB material of the CPMU, a temperature of 147K must be maintained. The CPMU is cooled using a LN<sub>2</sub> cryocooler and the magnet temperatures are maintained with heaters. The power the heaters add to the CPMU to maintain the temperature varies with electron beam fill. The power formula is trivial:  $P_{\text{beam heating}} = P_{\text{LN2 cryocooler}} - P_{\text{mag. heater}} - P_{\text{env. heat}}$ . The power of the LN<sub>2</sub> cryocooler is a direct function of how much nitrogen is boiled off, which is a constant. Therefore, any variation in the magnet heaters heat load is equal and opposite to the power deposited in the CPMU through electron beam heating.

### CPMU Results

Figure 2 shows that there is some evidence that heat load is related to SOCS and bunch length, although the 29% reduction in heat load predicted by moving from a 5 mm to a

7 mm gap is not evidenced. This indicates that evaluating the CPMU as a pair of infinite parallel plates is not an appropriate model of the device for beam heating purposes, and that a different model should be developed. The empirical heat load from a 900-bunch, 300 mA electron beam is also greater than the theoretical prediction, as with the wiggler data (Table 2).

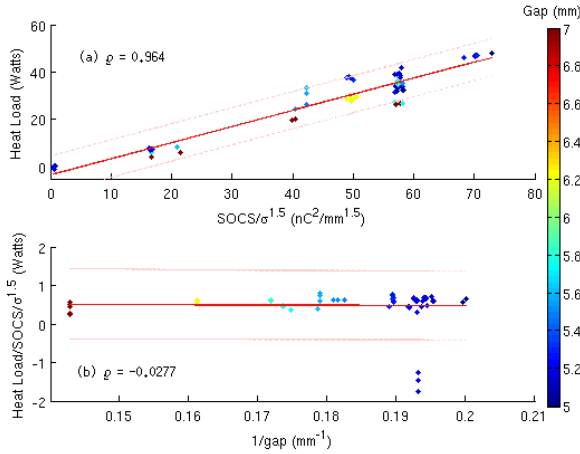


Figure 2: (a) Heat load vs. SOCS and (b) heat load/SOCS vs.  $1/\text{gap}$ . A relationship of heat load with SOCS is clear.

Table 2: Theoretical and Empirical Heat Loads on I12, I15, and the CPMU. The measured heat load on all three devices is greater than the theoretical predictions.

Device	Heat load (W) (900 bunch 300mA) theoretical	Heat load (W) (900 bunch 300mA) empirical
I12	0.809	4.52
I15	0.998	12.8
CPMU	8.677 <sup>1</sup>	66.15 <sup>2</sup>

<sup>1</sup> at 5 mm gap

<sup>2</sup> apparently gap independent

## ASSESSMENT OF THE PPM IN-VACS

In-vacuum IDs have temperature sensors attached to the aluminium magnet beams and on the copper foil tapers. Temperature sensing of the IDs has evolved over time: older IDs use Pt100s, whereas the newer devices utilise K-type thermocouples. The decay to background temperature is visible in the data when the electron beam is turned off. The temperature data around the time of a beam current drop to zero can be used to approximate heat load using Newton's Law of Cooling and the specific heat capacity equation:

$$\left. \frac{dQ}{dt} \right|_{t=0} = \frac{-mcT(0)}{\tau} \quad (7)$$

where  $Q$  is the heat loss,  $t$  is time,  $m$  is mass,  $c$  is the specific heat capacity,  $T(0)$  is the temperature at the start of the decay, and  $\tau$  is the time constant.

## J13 PPM In-Vac Results

The temperature data from the thermocouples analysed using the NSE model shows a correlation between heat loss and SOCS, when bunch length is taken into account. The correlation coefficient is fit to the data for small ID gaps only ( $< 8$  mm) for a more direct comparison to the wiggler and CPMU data. The data at large gaps do not appear to agree well with the small gap data.

In order to determine the absolute rate of cooling from the sensors, one major assumption is required: that the body the sensor is measuring is a uniform temperature. If this assumption is made for the aluminium beam holding the magnets, and the sensor is representative of a true uniform temperature, the cooling curve would imply electron beam heating in the tens of kilowatts. This is clearly unrealistic, instead we assume we are measuring a smaller uniform volume and report in arbitrary units. Therefore, the heat load should still vary with gap.

In accordance with the results for the CPMU, the cooling rate of J13 does not vary with the  $1/\text{gap}$  relationship expected from resistive wall heating (see Fig. 3). The lack of gap correlation supports the results given above for the CPMU: a new model is required for the CPMU and PPM in-vac devices.

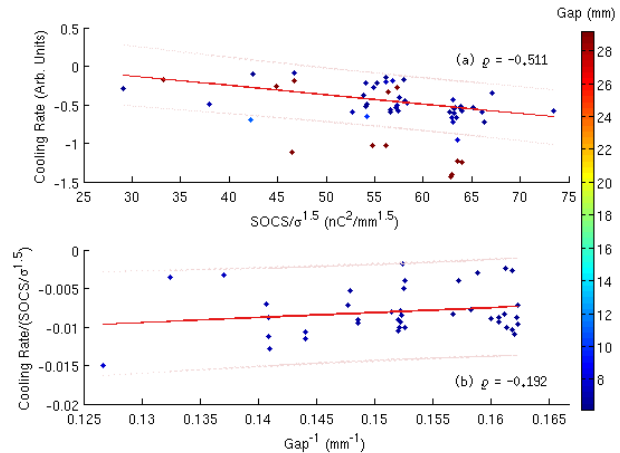


Figure 3: (a) Cooling rate vs. SOCS and (b) heat load/SOCS vs.  $1/\text{gap}$ . There is some evidence of a relationship between cooling rate vs. SOCS.

## SUMMARY

Accounting for bunch length when comparing the heat load of the SCWs with SOCS improves the fit of the data to models of resistive wall heating. However, the scatter in the data is still too large to determine if the image currents are active in the NSE or ASE regime. The CPMU and the PPM in-vac data have been compared against the NSE regime of resistive wall heating; the fit of the data improves once bunch length is taken into account, suggesting that the heating is indeed driven by RF effects. However, resistive wall heating should in principle vary inversely with ID gap, though no evidence was found to support this.

## REFERENCES

- [1] E. C. M. Rial and J. C. Schouten, “Electron Beam Heating Effects in Superconducting Wigglers at Diamond Light Source”, in *IPAC’10*, Kyoto, Japan, 2010, paper WEPD046, p. 3195.
- [2] J. C. Schouten and E. C. M. Rial, “Electron Beam Heating and Operation of the Cryogenic Undulator and Superconducting Wigglers at Diamond”, in *IPAC’11*, San Sebastián, Spain, 2011, paper THPC179, p. 3323.
- [3] Shi Cryogenics Group, 2012, [http://www.shicryogenics.com/wp-content/uploads/2012/11/RDK-408S2\\_Capacity\\_Map.pdf](http://www.shicryogenics.com/wp-content/uploads/2012/11/RDK-408S2_Capacity_Map.pdf)
- [4] A. Piwinski, “Longitudinal and Transverse Wake Fields in Flat Vacuum Chambers”, DESY, Hamburg, Germany, Rep. 84-097, 1984.
- [5] G. Reuter and E. Sondheimer, “The Theory of Anomalous Skin Effect in Metals”, *Proc. R. Soc. Lond. A*, vol. 195, no. 1042, pp. 336-364, 1948.
- [6] R. G. Chambers, “The Anomalous Skin Effect”, *Proc. R. Soc. Lond. A*, vol. 215, no. 1123, pp. 481-497, 1952.
- [7] E. C. M. Rial “A Summary of Electron Beam Heating in the DLS Superconducting Wigglers”, Diamond Light Source Ltd., Didcot, UK, Rep. TDI-ID-REP-081, Apr. 2013.
- [8] R. Walker, “Wigglers”, *CERN CAS*, Vols., 95-06, p. 807, 1995.